JACS
JOURNAL OF THE AMERICAN CHEMICAL SOCIETY

Communication

pubs.acs.org/JACS

Temperature-Dependent Dynamical Transitions of Different Classes of Amino Acid Residue in a Globular Protein

Yinglong Miao,[†,‡] Zheng Yi,[†,‡] Dennis C. Glass,[†,§] Liang Hong,[†] Madhusudan Tyagi,[∥,⊥] Jerome Baudry,[†,‡] Nitin Jain,[‡] and Jeremy C. Smith*[,†,‡]

[†]University of Tennessee/Oak Ridge National Laboratory Center for Molecular Biophysics, Oak Ridge National Laboratory, Oak Ridge, Tennessee 37831, United States

[‡]Department of Biochemistry and Cellular and Molecular Biology, University of Tennessee, Knoxville, Tennessee 37996, United States

[§]Graduate School of Genome Science and Technology, University of Tennessee, Knoxville, Tennessee 37996, United States

[∥]NIST Center for Neutron Research, National Institute of Standards and Technology, Gaithersburg, Maryland 20899, United States

[⊥]Department of Materials Science, University of Maryland, College Park, Maryland 20742, United States

Supporting Information

ABSTRACT: The temperature dependences of the nanosecond dynamics of different chemical classes of amino acid residue have been analyzed by combining elastic incoherent neutron scattering experiments with molecular dynamics simulations on cytochrome P450cam. At T = 100−160 K, anharmonic motion in hydrophobic and aromatic residues is activated, whereas hydrophilic residue motions are suppressed because of hydrogen-bonding interactions. In contrast, at T = 180−220 K, water-activated jumps of hydrophilic side chains, which are strongly coupled to the relaxation rates of the hydrogen bonds they form with hydration water, become apparent. Thus, with increasing temperature, first the hydrophobic core awakens, followed by the hydrophilic surface.

Proteins are dynamical entities that undergo a variety of internal motions spanning multiple time and length scales.[1] Neutron scattering has been widely applied to probe these motions on pico- to nanosecond time scales. For example, from elastic incoherent neutron scattering it is possible to extract the average mean square displacement (MSD) of protein nonexchangeable hydrogen atoms corresponding to motions that enter the resolution time scale of the neutron instrument.[2]

The temperature dependence of internal protein dynamics provides fundamental information on the corresponding energy landscape. Previous elastic neutron scattering studies have revealed two transitions in the temperature dependence of the protein MSD.[3,4] A first nonlinear increase appears at T = 100−150 K and has been attributed to the activation of methyl group rotations.[5,6] This transition is independent of protein hydration.[6] The second transition appears at T = 180−220 K and is hydration-dependent, being driven by the translational diffusion of water molecules on the protein surface.[7−9] The higher-temperature transition has also been detected by a variety of other experimental techniques, such as Mössbauer spectroscopy,[10] optical absorption spectroscopy,[11] and X-ray diffraction.[12]

To understand further the molecular origin of the two protein transitions, we performed elastic incoherent neutron scattering on camphor-bound cytochrome P450 (P450cam)[2] and carried out molecular dynamics (MD) simulations to interpret the results [see the Supporting Information (SI) for experimental and simulation details]. We examined separately the scattering of nonexchangeable hydrogen atoms in the protein arising from the backbone and hydrophilic (charged and polar), hydrophobic, and aromatic side chains (Figure 1a) and systematically analyzed their individual contributions to the two protein transitions.

Using the high-flux backscattering (HFBS) spectrometer at the National Institute of Standards and Technology (NIST) with ∼1 μeV energy resolution, corresponding to a time scale of ∼1 ns, we performed elastic incoherent neutron scattering experiments on P450cam in both the dry powder form and in hydrated powder forms with hydrations (h) of 0.05 and 0.4 g of D_2O/g of protein (hereafter denoted as "h = 0.05" and "h = 0.4", respectively). The average protein MSDs and the corresponding variances σ^2 (Figure S1 in the SI) were obtained by applying a q^4 fitting algorithm presented previously.[2] As shown in Figure 1b, the first deviation from linearity of the protein average MSD as a function of temperature was observed at T = 140−160 K, and in the hydrated sample only, the second appeared at T = 180−220 K. In parallel with the experiments, MD simulations were performed on both the dry and hydrated powder forms of P450cam (Figure S2) at temperatures from 300 to 10 K at 10 K intervals. The MSDs of nonexchangeable hydrogen atoms in the protein calculated from the MD simulations on the 1 ns time scale agreed quantitatively with the experimental data in the low-T regime and were slightly higher than the experimental values at higher temperatures (T > 180 K) by 25 ± 7 and 14 ± 6% for the dry and hydrated P450cam, respectively (Figure 1b). Similar to the experimental observations, the simulation-derived MSDs exhibited one transition at $T \approx$ 150 K and another for only the hydrated sample at T = 180−220 K. The ratio of the MSD slope of hydrated P450cam to that of the dry sample at 220 K < $T \leq$ 300 K obtained from the simulations was 1.53, in good agreement with the value of 1.57 from the experimental data.

Received: October 3, 2012
Published: November 9, 2012

   dx.doi.org/10.1021/ja3097898 | J. Am. Chem. Soc. 2012, 134, 19576−19579

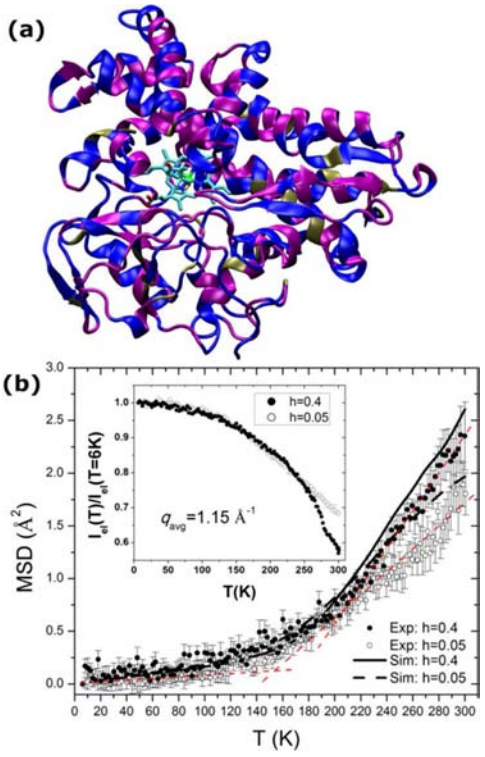

Figure 1. (a) X-ray crystal structure of P450cam with hydrophilic, hydrophobic, and aromatic residues colored in blue, purple, and green, respectively. The heme and camphor are represented in licorice. (b) MSDs of P450cam in $h = 0.4$ and $h = 0.05$ powder calculated from MD simulations at 1 ns compared with those obtained on the HFBS spectrometer with 1 μeV resolution. Red dashed lines are linear fits to the experimental data for $h = 0.05$ protein at $T < 100$ K and both $h = 0.05$ and hydrated $h = 0.4$ protein at 220 K $< T \leq$ 300 K. Inset: Experimentally measured elastic intensities used to extract the protein MSDs.

Next, using the MD simulations, we investigated the contributions to the two dynamic transitions made by different residue types in the protein. The MSD for rotations of the methyl groups was calculated as the difference between the MSD of the hydrogen atoms in the methyl groups from the original MD trajectory and that of a trajectory with methyl rotations removed.[13] The methyl rotations were found to exhibit a hydration-independent transition at $T \approx 150$ K (Figure S3), in agreement with previous interpretations.[5,6] In contrast, the MSD calculated for the protein backbone hydrogen atoms was found to increase linearly over the entire temperature range in the dry sample but to exhibit a clear transition at $T = 180-220$ K in the hydrated system (Figure 2). A previous study of a glycine polypeptide with only backbone hydrogen atoms showed a similar hydration-dependent dynamical transition.[14]

We divided the side chains into charged [Arg, Lys, seven doubly protonated His (17, 21, 80, 176, 308, 337, and 355), and all Asp and Glu except the protonated Asp297 and Glu366[2,15]], polar (Ser, Thr, Asn, Gln, Cys, Tyr, protonated Asp297 and Glu366, and all His except the seven doubly protonated ones), hydrophobic (Ala, Leu, Ile, Val, Met, and Pro), and aromatic (Phe and Trp) residues. For all of these calculations, the methyl rotations were removed. The nonexchangeable hydrogen atoms from the charged and polar side chains exhibited closely similar MSD versus T profiles (Figure S4) and were therefore combined into one class, denoted as "hydrophilic". Of the total of 2520 nonexchangeable hydrogen atoms in P450cam, 17.4, 31.5, 44.7,

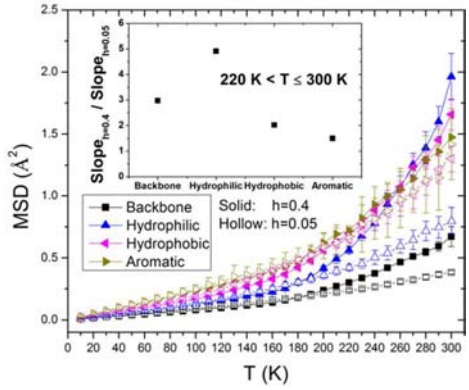

Figure 2. Decomposition of the MSD of protein nonexchangeable hydrogen atoms into contributions from the backbone and the hydrophilic, hydrophobic, and aromatic side chains. Methyl rotations have been removed. Inset: ratios of MSD-vs-T slopes at $h = 0.4$ and $h = 0.05$ in the temperature regime 220 K $< T \leq$ 300 K.

and 6.4% belong to the backbone and the hydrophilic, hydrophobic, and aromatic side chains, respectively.

The MSDs calculated for the above classes of residue are plotted in Figure 2. Interestingly, in the dry protein and at $T \leq$ 220 K in the $h = 0.4$ hydrated protein, the hydrophilic residues exhibited a lower average MSD than both the hydrophobic and aromatic residues. The gradient of MSD versus T was computed over three temperature regimes (see Table S1 in the SI). Below $T \approx 150$ K, the MSD slopes in the hydrated $h = 0.4$ protein were similar to those in the dry protein. However, above $T \approx 220$ K, the slopes increased by factors of 1.5−5 upon protein hydration (Figure 2), with the hydrophilic side chains exhibiting the largest increase, from 3.79×10^{-3} to 1.86×10^{-2} Å^2/K. Hence, the hydrophilic residues have the strongest hydration dependence. This finding is consistent with an earlier study of tyrosine residues (categorized here as hydrophilic) in bacteriorhodopsin, which were found to exhibit MSDs smaller than the average for the entire membrane in the intermediate-T regime (120−250 K) but larger than the average in the high-T regime ($T > 250$ K), with the corresponding slope being greater than those for both isoleucine and leucine residues.[16]

To characterize further the temperature-dependent dynamics of the different residue types, we decomposed the motions of the hydrogen atoms in the protein following the method in ref 13. In this approach, scatter plots of individual hydrogen atom trajectories are represented as clusters corresponding to energy wells. Hydrogen atoms diffuse locally within the wells and jump between them. The number of energy wells (minima) averaged over the hydrogen atoms revealed that after exclusion of the methyl rotations, the hydrophobic side chains still exhibit a low-T transition at $T = 100-150$ K, a temperature range similar to that observed for the onset of methyl rotations (Figure 3a). Moreover, this transition is nearly hydration independent. In contrast, the hydrophilic side-chain jumps are activated at a higher temperature ($T \approx 160$ K) and are strongly dependent on protein hydration above $T \approx 220$ K. Overall, in both the dry and hydrated samples, hydrogen atoms in the hydrophilic side chains undergo fewer jumps than those in the hydrophobic groups. The aromatic side chains follow the hydrophilic side chains for temperatures below $T \approx 220$ K but do not exhibit the hydration-driven high-T effect.

The jump distances of the nonexchangeable hydrogen atoms are similar to those calculated in a previous study of lysozyme and

dx.doi.org/10.1021/ja3097898 | J. Am. Chem. Soc. 2012, 134, 19576−19579

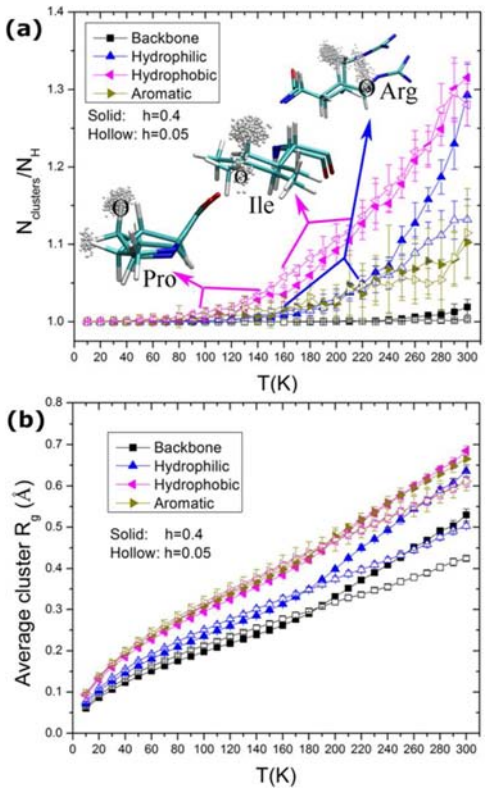

Figure 3. Temperature dependences of (a) the average number of clusters per hydrogen atom and (b) the average cluster radius of gyration calculated for nonexchangeable hydrogen atoms in different types of residue. The insets in (a) show example jumps of nonexchangeable hydrogen atoms in Pro, Ile, and Arg side chains, as labeled.

are also hydration-independent.[17] Furthermore, the jump distances are similar for hydrogen atoms of different residue types (see Figure S5b). The radius of gyration (R_g) of a scatter-plot cluster for an individual hydrogen atom corresponds roughly to the accessible radius of the corresponding energy well. The average R_g values of the scatter-plot clusters of nonexchangeable hydrogen atoms in the different residue types are shown in Figure 3b. All of the residue types were found to exhibit a hydration-dependent transition at $T \approx 180$ K, with a significantly stronger hydration dependence observed for the hydrophilic residues. At 300 K, the ratios of R_g at $h = 0.4$ to that at $h = 0.05$ were 1.26, 1.12, and 1.09 for the hydrophilic, hydrophobic, and aromatic groups, respectively.

For the transition observed at $T \approx 150$ K in the hydrophobic side chains, further analysis revealed that this originates mainly from jumps of hydrogen atoms in the proline side chains (see the inset for Pro in Figure 3a). The five-membered ring in proline can adopt two distinct conformations, down-puckered (C_γ-endo) or up-puckered (C_γ-exo), which are roughly equally populated in protein crystal structures.[18] The energy barrier is ~3 kcal/mol in the CHARMM force field, and the strain in the $C_\gamma-C_\delta-N$ angle potential has been suggested to be the principal barrier between these two conformations.[19] Similarly, quantum-chemical calculations have estimated the barriers for the proline puckering transition in water to be 3.1 and 3.0 kcal/mol for the trans and cis conformers, respectively.[20] This energy barrier is closely similar to that for methyl rotations (~3 kcal/mol),[13,21,22] consistent with the presence of these jumps on similar time scales and temperatures as methyl rotations.

Jumps of nonexchangeable hydrogen atoms in aromatic phenyl rings and the methylene groups ($-CH_2-$) that are not in proline side chains enter the 1 ns time window at higher temperatures ($T = 160-220$ K) (Figure 3a). Example hydrogen jumps in Ile and Arg side chains due to dihedral transitions involving the $-CH_2-$ group are shown as insets in Figure 3a. Similar motions were observed in other side chains of those residues that contain $-CH_2-$ groups, such as Leu, Met, Lys, Glu, and Asp. Jumps of hydrogen atoms in aromatic phenyl rings are illustrated in Figure S5a. This jump also arises from dihedral angle rotations related to the $-CH_2-$ group in the side chain.

To quantify the relative contributions of the above protein motions to the low-T transition, we compared the total MSD for jumps of nonexchangeable hydrogen atoms with those of the methyl rotations and the proline puckering, all quantities being weighted by the corresponding number of hydrogen atoms involved (see the SI for details). The results showed a ~0.38 Å^2 increase in the total MSD of hydrogen jumps from 100 to 220 K, to which methyl rotations contributed ~0.32 Å^2 and proline puckerings ~0.04 Å^2 (Figure S6). Hence, methyl rotations contribute ~85% and proline puckerings ~10% to the low-T transition, with the remaining ~5% arising from hydrogen motions in aromatic phenyl rings and those $-CH_2-$ groups not in proline side chains. In a previous experimental study of homomeric polypeptides,[14] motions of non-methyl groups (the phenyl ring and methylene groups) were indirectly inferred to contribute 10–20% to the low-T transition, a fraction similar to the present results.

To understand the origin of the lower MSDs of the hydrophilic side chains in both the dry protein and the $h = 0.4$ hydrated protein at $T \leq 220$ K relative to those of the hydrophobic and aromatic residues (Figure 2), we analyzed hydrogen bonds formed between the hydrophilic side chains and the neighboring protein residues and hydration water. There are 202 hydrophilic residues in total in P450cam. In the dry-protein simulations, each hydrophilic side chains forms ~1.8 hydrogen bonds on average with neighboring protein residues, and these hydrogen bonds appear to be stable over the entire temperature range (Figure S7a). A previous study of charged residues in P450cam also revealed stable salt bridges (32 out of the total of 53 ionic pairs) in the protein.[23] These salt-bridge and hydrogen-bonding interactions significantly restrict the motions of the hydrophilic side chains, which are important in regulating substrate binding.[22,23] Furthermore, in the dry and $h = 0.05$ proteins, the hydrophilic side chains form an average of ~0.8 hydrogen bonds with the small amount of hydration water, which itself exhibits a lower MSD at $T \leq 220$ K as a result of the arrest of water translational degrees of freedom near the glass transition temperature, $T_g \approx 170$ K[25,27] (Figure S7b). In contrast, the hydrophobic and aromatic residues clearly make no hydrogen-bonding interactions with the hydration water. Analysis of the simulations of the $h = 0.4$ hydrated protein similarly showed stabilization of the hydrophilic side chains at $T \leq 220$ K by the hydrogen-bonding interactions with neighboring residues and hydration water. Consequently, the hydrophilic side-chain hydrogen atoms undergo fewer jumps and localized diffusion of smaller magnitude, as shown in Figure 3, leading to lower MSD values than for the hydrophobic and aromatic residues.

To understand the strong hydration dependence of the dynamics of the hydrophilic side chains at high T, and especially their jumps, we compared the MSDs of the hydration water in the dry and hydrated P450cam simulations with k_R, the rate constant for relaxation of the hydrogen bonds formed between

dx.doi.org/10.1021/ja3097898 | J. Am. Chem. Soc. 2012, 134, 19576–19579

the hydrophilic side chains and the water molecules. The k_R values were calculated as the reciprocals of the average relaxation times (τ_R) determined from the decay of the hydrogen-bond correlation function $c(t) = \langle h(t)h(0)\rangle/\langle h\rangle$, where $h(t)$ is a hydrogen-bond population operator with a value of 1 if a given donor−acceptor pair is hydrogen-bonded at time t and zero otherwise, and $\langle\cdots\rangle$ denotes the ensemble average over all donor−acceptor pairs.[7,24] As shown in Figure 4, at $T > 180$ K, the

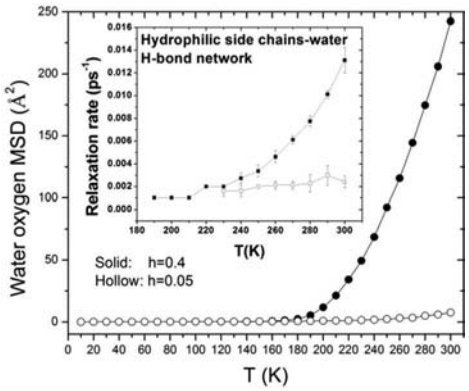

Figure 4. Plots of MSD vs T for hydration water in the $h = 0.4$ and $h = 0.05$ hydrated proteins. The inset shows plots of the associated relaxation rates of the hydrogen-bond networks formed between the hydrophilic side chains and the hydration water.

hydration water underwent significantly greater translational dynamics in the hydrated $h = 0.4$ simulation than in the $h = 0.05$ simulation. Concurrently, there was a clear transition in the hydrogen-bond network relaxation rate at $T \approx 220$ K in the hydrated $h = 0.4$ protein that was not present in the dry protein. This coincides with the hydration-dependent transition in jumps of the hydrophilic groups observed in Figure 3a. This finding agrees with the results of previous studies showing that the onset of protein dynamical transitions largely depends on the fluctuations of protein−water hydrogen bonds[25,26] and that transitions in the k_R of hydrogen bonds between hydration water and the entire protein and in the protein MSD occur concomitantly at $T \approx 220$ K;[7,27] furthermore, it pinpoints the effect of the protein hydration dependence as being primarily on the hydrophilic groups and not the hydrophobic or aromatic groups.

In conclusion, analysis of the temperature dependence of different classes of amino acid residue has revealed the following picture of changes in nanosecond protein dynamics with increasing temperature. As the temperature is increased from the harmonic regime ($T < 100$ K), proline puckering transitions and methyl rotations are activated. Jumps of nonexchangeable hydrogen atoms in the non-proline methylene groups and aromatic phenyl rings enter the 1 ns time window at $T = 160$−220 K. For $T \leq 220$ K, protein flexibility arises from the hydrophobic and aromatic residues, which are dynamically activated, in contrast to the hydrophilic residues, the dynamics of which are suppressed as a result of stable hydrogen bonding interactions with the neighboring protein residues and hydration water. As T is further increased, at $T \approx 180$−220 K, strongly hydration-dependent increases in the localized diffusion of protein nonexchangeable hydrogen atoms and jumps in the hydrophilic side chains are found. Finally, the jumps in hydrophilic side chains are strongly coupled to the relaxation rates of the hydrogen bonds formed with hydration water.

■ ASSOCIATED CONTENT

Supporting Information

Details of the sample preparation, neutron scattering experiments, and MD simulations. This material is available free of charge via the Internet at http://pubs.acs.org.

■ AUTHOR INFORMATION

Corresponding Author

smithjc@ornl.gov

Notes

The authors declare no competing financial interest.

■ ACKNOWLEDGMENTS

This project was supported by the National Science Foundation (NSF) (Award MCB-0842871). Computing time on the Kraken supercomputer and on the Franklin and Hopper supercomputers was provided in part by a NSF TeraGrid Award (Grant TG-MCA08X032) and a National Energy Research Scientific Computing Center (NERSC) Award (Project M906), respectively. This work utilized facilities supported in part by NSF under Agreement DMR-0944772.

■ REFERENCES

(1) Henzler-Wildman, K.; Kern, D. *Nature* **2007**, *450*, 964.
(2) Yi, Z.; Miao, Y. L.; Baudry, J.; Jain, N.; Smith, J. C. *J. Phys. Chem. B* **2012**, *116*, 5028.
(3) Doster, W.; Cusack, S.; Petry, W. *Nature* **1989**, *337*, 754.
(4) Zaccai, G. *Science* **2000**, *288*, 1604.
(5) Krishnan, M.; Schulz, R.; Smith, J. C. *AIP Conf. Proc.* **2009**, *1102*, 122.
(6) Roh, J. H.; Curtis, J. E.; Azzam, S.; Novikov, V. N.; Peral, I.; Chowdhuri, Z.; Gregory, R. B.; Sokolov, A. P. *Biophys. J.* **2006**, *91*, 2573.
(7) Wood, K.; Frolich, A.; Paciaroni, A.; Moulin, M.; Hartlein, M.; Zaccai, G.; Tobias, D. J.; Weik, M. *J. Am. Chem. Soc.* **2008**, *130*, 4586.
(8) Tournier, A. L.; Xu, J. C.; Smith, J. C. *Biophys. J.* **2003**, *85*, 1871.
(9) Zaccai, G. *Philos. Trans. R. Soc., B* **2004**, *359*, 1269.
(10) Parak, F. G. *Rep. Prog. Phys.* **2003**, *66*, 103.
(11) Melchers, B.; Knapp, E. W.; Parak, F.; Cordone, L.; Cupane, A.; Leone, M. *Biophys. J.* **1996**, *70*, 2092.
(12) Rasmussen, B. F.; Stock, A. M.; Ringe, D.; Petsko, G. A. *Nature* **1992**, *357*, 423.
(13) Hong, L.; Smolin, N.; Lindner, B.; Sokolov, A. P.; Smith, J. C. *Phys. Rev. Lett.* **2011**, *107*, No. 148102.
(14) (a) Schiro, G.; Caronna, C.; Natali, F.; Cupane, A. *J. Am. Chem. Soc.* **2010**, *132*, 1371. (b) Schiro, G.; Caronna, C.; Natali, F.; Cupane, A. *Phys. Chem. Chem. Phys.* **2010**, *12*, 10215.
(15) Miao, Y.; Baudry, J. *Biophys. J.* **2011**, *101*, 1493.
(16) Wood, K.; Grudinin, S.; Kessler, B.; Weik, M.; Johnson, M.; Kneller, G. R.; Oesterheit, D.; Zaccai, G. *J. Mol. Biol.* **2008**, *380*, 581.
(17) Hong, L.; Cheng, X. L.; Glass, D. C.; Smith, J. C. *Phys. Rev. Lett.* **2012**, *108*, No. 238102.
(18) Vitagliano, L.; Berisio, R.; Mastrangelo, A.; Mazzarella, L.; Zagari, A. *Protein Sci.* **2001**, *10*, 2627.
(19) Ho, B. K.; Coutsias, E. A.; Seok, C.; Dill, K. A. *Protein Sci.* **2005**, *14*, 1011.
(20) Kang, Y. K. *J. Phys. Chem. B* **2007**, *111*, 10550.
(21) Xue, Y.; Pavlova, M. S.; Ryabov, Y. E.; Reif, B.; Skrynnikov, N. R. *J. Am. Chem. Soc.* **2007**, *129*, 6827.
(22) Miao, Y.; Yi, Z.; Cantrell, C.; Glass, D.; Baudry, J.; Jain, N.; Smith, J. C. *Biophys. J.* **2012**, DOI: 10.1016/j.bpj.2012.10.013.
(23) Lounnas, V.; Wade, R. C. *Biochemistry* **1997**, *36*, 5402.
(24) Luzar, A.; Chandler, D. *Nature* **1996**, *379*, 55.
(25) Doster, W.; Busch, S.; Gaspar, A. M.; Appavou, M. S.; Wuttke, J.; Scheer, H. *Phys. Rev. Lett.* **2010**, *104*, No. 098101.
(26) Doster, W.; Settles, M. *NATO Sci. Ser., Ser. A* **1999**, *305*, 177.
(27) Tarek, M.; Tobias, D. J. *Eur. Biophys. J.* **2008**, *37*, 701.